Journal of Nanoscience and Nanoengineering
Vol. 5, No. 1, 2019, pp. 1-6
http://www.aiscience.org/journal/jnn
ISSN: 2471-8378 (Print); ISSN: 2471-8394 (Online)

Fabrication of Electrode TiO_2 Nanofibers for Hydrogen Generation from Photoelectrochemical Water Splitting

Van Nghia Nguyen[1, 2], Manh Son Nguyen[2], Minh Thuy Doan[1], Nhat Hieu Hoang[1, *]

[1]Department of Physics, Quy Nhon University, Quy Nhon City, Viet Nam
[2]Department of Physics, Hue University of Sciences, Hue City, Viet Nam

Abstract

TiO_2 nanofibers (NFs) structures were fabricated on the indium tin oxide (ITO) conducting substrates that serve as working electrodes in photoelectrochemical (PEC) cells for the generation of hydrogen by water splitting. The TiO_2-NFs were synthesized by the electrospinning method at room temperature using the spray solution of Titanium tetraisopropoxide and Polyvinylpyrrolidone polymer at different times spraying to optimize the water splitting efficiency. The samples were characterized by X-ray diffraction (XRD), scanning electron microscopy (SEM), transmission electron microscopy (TEM), X-ray photoelectron spectroscopy (XPS). The photoelectrochemical (PEC) properties of the electrodes were measured, using a three-electrodes electrochemical analyzer illuminated with a standard 150W Xenon lamp. It was found that maximum water splitting efficiency of TiO_2-NFs electrode with spraying time at 20 min was about 0.03% (corresponding photocurrent density 80 μA/cm^2 at V_{bias} = 0.2 V). This result is relatively higher compared to TiO_2 nanostructures in previous studies.

Keywords

Water Splitting, TiO_2 Nanofiber, Photoelectrochemical Cell, Electrospinning, Nanomaterials

Received: January 28, 2019 / Accepted: March 14, 2019 / Published online: April 10, 2019

1. Introduction

Fossil fuels such as coal, oil and gas have become a major source of energy for power generation in many countries around the world. However, these energy sources are also gradually exhausting, which makes developing clean and renewable energies a very important task. Hydrogen is widely considered to be the fuel of the future because of the fossil fuels increased price and its environmentally friendly nature. There is a growing awareness that hydrogen could reduce the dependence on imported oil and avoid the next potential energy crisis, driven by the actual dependence of existing societies to oil producer countries. Hydrogen is environmentally safe when it is generated from renewable sources like wind, hydroelectric, tidal, geothermal, or solar energies [1-3]. The water splitting in a photoelectrochemical cell (PEC) is a promising way for hydro production. It is environmentally safe, with no undesirable by-products, and is easy to achieve [4]. Therefore, hydrogen is an attractive alternative energy source that addresses several energy availability and environmental issues.

Among the semiconductor used in the photoelectrochemical field, Titanium dioxide (TiO_2) has been selected for the present investigation because it represents a good compromise between stability to corrosion and photocorrosion, as well as having a low cost, a high availability, and a low toxicity [5].

* Corresponding author
E-mail address: hieuktvl@yahoo.com (N. H. Hoang)

The first study on the process of water separation using TiO_2 was made by Fujishima and Honda in 1972 [6]. Most of these early water-splitting studies focused on TiO_2 nanostructured nanoparticles because they exhibit many great advantages for photocatalysts, adsorbers or sensors, due to their large surface area and ease of manufacture [7-9]. However, the use of TiO_2 0D still has drawbacks such as fast recombination of electrons and holes, slow charge transfers, and high recycling costs that limit its photocatalytic efficiency [1].

In recent years, One-dimensional (1D) nanostructured materials have become one of the hottest research fields because the anisotropic morphology of one-dimensional (1D) nanostructure makes it exhibit superior optical, magnetic, electrical, and mechanical properties [10]. One-dimensional (1D) TiO_2 nanostructures, such as nanorods, nanofibers, and nanotubes were successfully synthesized. Nanofiber structure is a promising photocatalyst because of high activities and large surface area. Many methods such as sol-gel [11], electrospinning [12], electrochemical anodization [13], laser pulse deposition [14], or hydrothermalism [15] have been utilized for the synthesis of nanofiber TiO_2. Among the methods for preparing nanomaterials, electrospinning has attracted much attention because it provides a cost-effective, versatile, simple and continuous process. The principle of electrospinning is to apply high voltage on a syringe needle connected to another syringe containing a polymer solution. When the polymer solution flows out from the needle, the polymer is pulled onto a collector by strong electric field and forms a nanofiber structure. In this study, Polyvinyl-pyrrolidone/TiO_2 nanofibers is prepared by electrospinning in combination with calcination. The thickness of TiO_2 deposited on ITO is controlled to optimize the photoconversion efficiency.

2. Experimental

2.1. Preparation of TiO_2 Nanofibers

The TiO_2 nanofibers were fabricated by electrospinning a mixture of TiO_2 sol and Polyvinylpyrrolidone (PVP) (*M*w ~ 360.000, Sigma-Aldrich) polymer. First, the TiO_2 sol was prepared by hydrolyzing 3 mL of Titanium tetraisopropoxide [Ti(O*i*Pr)$_4$; 97%, Sigma-Aldrich] with a mixture of 5 mL of Ethanol (98%) and 3 mL of Acetic acid (99%). Next, PVP was separately dissolved in 5 mL of Ethanol and then added to the TiO_2 sol solution. The precursor mixture was stirred for 2 hours at room temperature to have the required viscosity for electrospinning. The precursor solution was then filtered to remove possible impurities. The solution was then placed in a 5 mL syringe attached to the syringe pump and fed into the metal needle. The precursor solution was then electrospun under conditions of applied voltage (kV) and flow rate (mL/h) of 10 kV and 0.04 mL/h. The ITO conducting substrates (2.5×2.5 mm) were placed on a grounded collector for the accumulation of NFs. After collecting times, the electrode was dried in the air for 5 hours to allow the hydrolysis of Ti(OiPr)$_4$. Finally, the Ti(OiPr)$_4$/PVP composite nanofibers were oxidized for 3 hours at 500°C with a heating rate of 2°C/min in ambient atmosphere to remove the PVP and form the TiO_2-NFs on ITO substrate. The thickness of TiO_2-NFs deposited on ITO is controlled by changing the collecting time. The spraying times were 5 min, 10 min, 15 min, 20 min and 25 min. The electrodes corresponding to 25 min was flaked away after sintering. Because the TiO_2 layer was too thick, we could not investigat the properties of this electrode.

2.2. Film Characterization

The morphology of the fabricated structures were examined by field-emission scanning electron microscopy (FE-SEM; Hitachi S4800), High-resolution transmission electron microscopy (HRTEM; JEOL JEM-2100F), and X-ray diffraction (XRD, Siemen D5005) using Cu Kα radiation with Ni filter with a step size of 0.02°. The elemental and chemical states analysis were determined by X-ray photoelectron spectroscopy (XPS) (GT-3000A).

2.3. Photoelectrochemical Measurements

PEC properties were measured with a three-electrodes electrochemical analyzer (Model DY2300), using the fabricated nanostructure films formed on ITO as the working electrode, a platinum (Pt) wire as the counter electrode, and Ag/AgCl in saturated KCl as the reference electrode. The electrolyte utilized for the TiO_2 structures consists of 0.5 M Na_2SO_4. A 150 W Xe lamp (Gloria – X150A) was used as a simulated sunlight source with an intensity of 100 mW/cm^2 to evaluate the photon-to-current conversion efficiency of the photoanodes. All the measurements were performed with front-side illumination of the photoanodes and the linear sweep potential at a scan rate of 50 mV/s. The exposed area of the working electrode to the electrolyte was fixed at 1 cm^2 using nonconductive epoxy resin. The electrode performance was evaluated via the photoconversion efficiency measurement using the following equation [1]:

$$\eta(\%) = J_p(E_{rev} - E_{app})*100/I_o$$

where J_p is the measured photocurrent density (mAcm^{-2}), I_o is the incident light intensity of the solar simulator (100 mW/cm^2), E_{rev} is the standard state-reversible potential (1.23V), E_{app} (= E_{meas} - E_{aoc}) is the applied potential, in which E_{meas} is the electrode potential (*vs* Ag/AgCl) of the working electrode under illumination, and E_{aoc} is the electrode potential (*vs* Ag/AgCl) of the same working electrode under open circuit conditions [16].

3. Results and Discussion

3.1. Structural Studies

Figure 1 shows that the XRD patterns of the prepared samples calcined at 500°C for 3 hours in air atmosphere with spraying time 15 min and 20 min, respectively. The patterns indicate the presence of anatase TiO_2 structure with peaks at 2θ = 25.3° and 38.56°, corresponding to the diffraction on the (101) and (112) planes of anatase TiO_2. The peak values we measured are consistent with the JCPDS (file no. 84-1286) diffraction patterns of the anatase TiO_2.

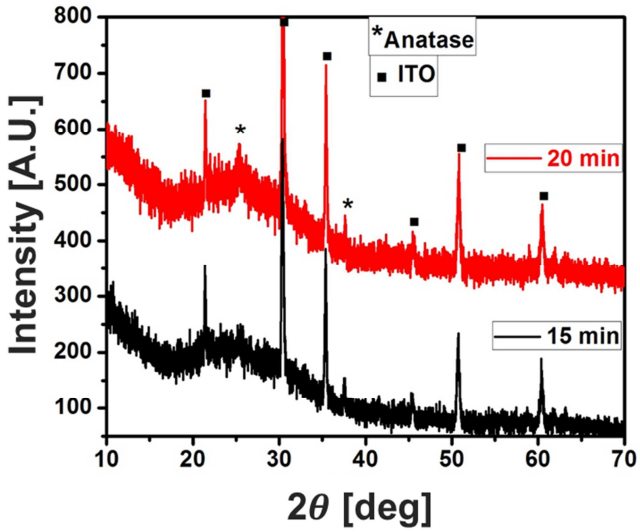

Figure 1. XRD patterns of the prepared samples calcined at 500°C.

The Raman spectra recorded was used to confirm the anatase structure of the TiO_2. Figure 2 shows the Raman spectra (RFS 100 FT-Raman Bruker spectrometer) of different times spraying. The spectra were taken at room temperature using a 632.8 nm laser line as the excitation source. In particular, anatase has six Raman active modes. In the case of anatase single crystal, six bands in the first-order Raman spectrum were identified at 144 cm^{-1} (Eg), 197 cm^{-1} (Eg), 399 cm^{-1} (B1g), 513 cm^{-1} (A1g), 519 cm^{-1} (B1g), and 639 cm^{-1} (Eg) [17]. Vibration peaks at 399 cm^{-1} (B1g), 513 cm^{-1} (A1g) and 639 cm^{-1} (Eg) are present in the spectra for all samples, which indicates that anatase TiO_2 crystalline are the predominant species. Furthermore, different peaks were not observed. This is in good agreement with the results of XRD spectrum.

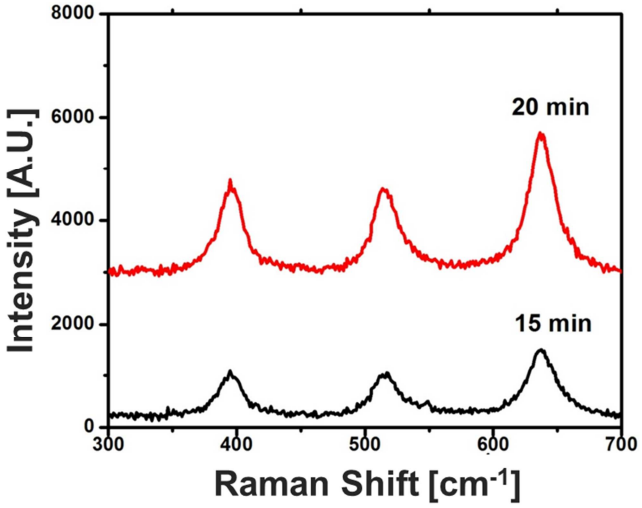

Figure 2. Raman spectra of the prepared samples calcined at 500°C.

3.2. Morphological Studies

The morphologies of the prepared PVP/TiOPr composite nanofibers and TiO_2 nanofibers are shown in Figure 3.

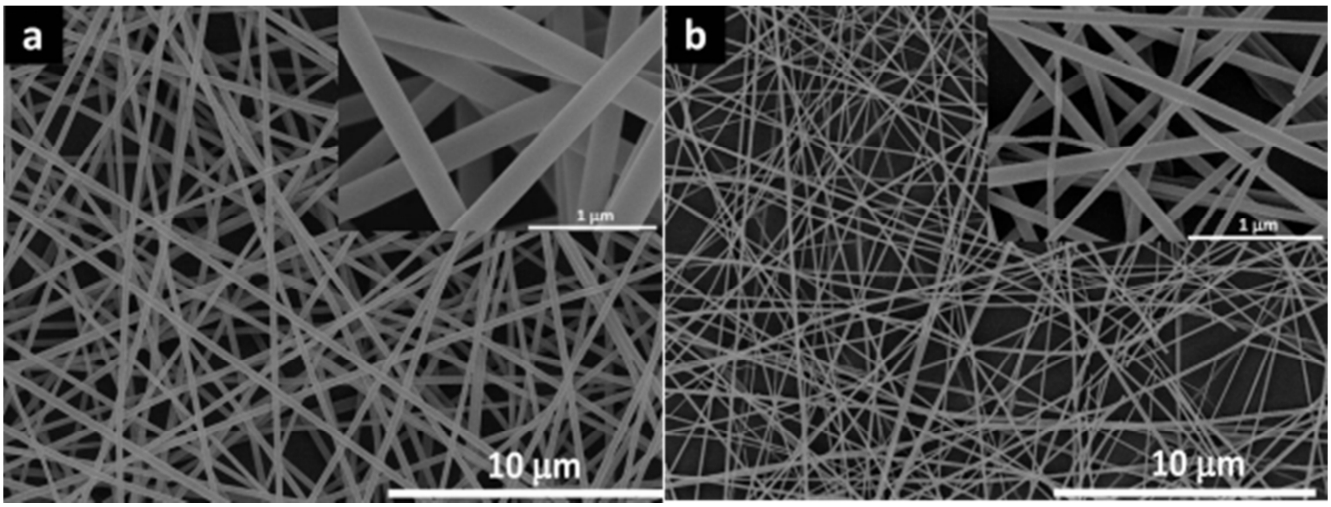

Figure 3. SEM images of the samples (a) PVP/TiOPr composite nanofibers, (b) TiO_2 nanofibers sintered at 500°C.

It is clearly observed that the PVP/TiOPr composite nanofibers formed a fibrous structure with varying fiber diameters, as revealed in Figure 3a. The electrospun PVP/TiOPr composite nanofibers showed smooth surface, with fiber diameters ranging from 200 nm to 550 nm. The calcinations significantly altered the surface morphologies of

the electrospun nanofibers, as presented in Figure 3b. It is evident that the diameters of the corresponding TiO_2 nanofibers got smaller than the electrospun ones, after calcination process. The diameters of TiO_2 nanofibers ranged from 200 to 350 nm for nanofibers obtained at 500°C and the length of NFs is in the range of hundreds of micrometers. TiO_2 nanofibers were composed of TiO_2 nanoparticles, aggregated along fiber orientation.

Figure 4 shows the HRTEM and EDS used to prove the crystalline phase. Figure 4a showed the TEM picture of TiO_2-NFs, the diameter of NFs corresponded to the result of SEM. The EDX spectrum (inset Figure 4a) had the two peaks of Ti, O and no different peaks were observed (the peak of C was grid carbon when measuring samples). The HR-TEM images of the TiO_2-NFs show a highly crystalline structure in which the lattice fringes of TiO_2 are clearly visible. Accordingly, a lattice constant of 0.35 nm was determined for TiO_2, which corresponds to the lattice spacing between the (101) planes of the anatase TiO_2 (JCPDS file no. 84-1286). These results are in good agreement with the results obtained by XRD, as shown in Figure 1.

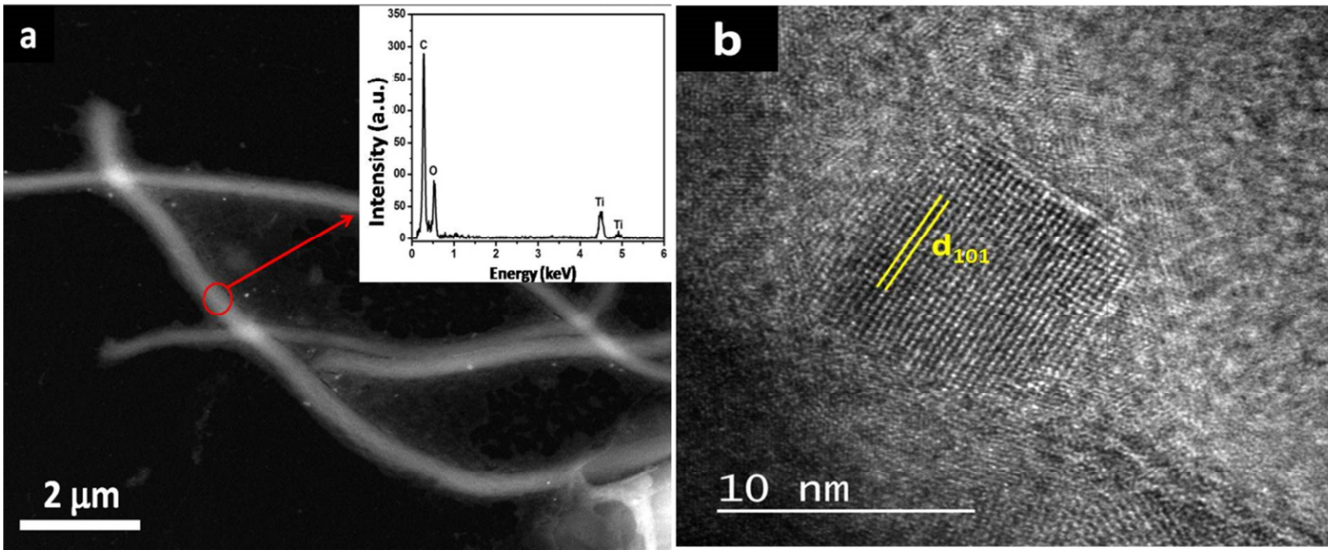

Figure 4. The TEM (a) and HR-TEM (b) images of TiO_2-NFs with a spraying time of 20 min.

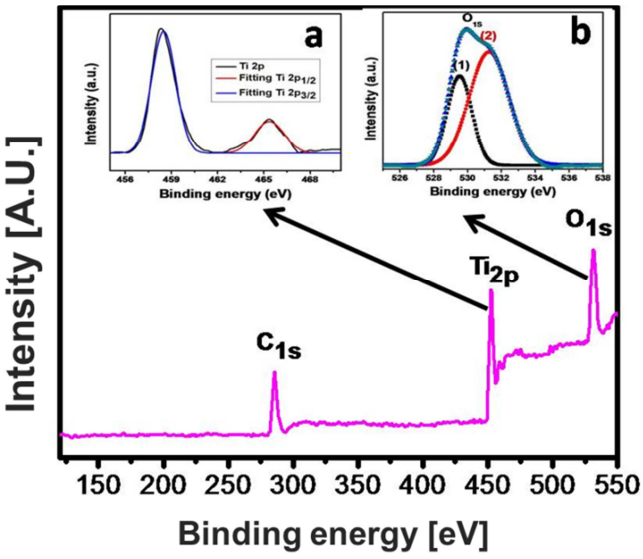

Figure 5. XPS spectra of sample: the whole survey spectrum of TiO_2-NFs in set Ti 2p peak (a) the O 1s peak (b).

To investigate the surface chemical compositions and the valence states of the elements existing in the sample, XPS measurements were performed on the TiO_2-NFs. The spectrum of figure 5 indicates the presence of Ti and O elements in the sample. The peak created by the spin - orbital interaction for Ti 2p producing the doublet Ti $2p_{3/2}$ and Ti $2p_{1/2}$ can be observed in inset Figure 5a. The peaks at 465 eV and 458.6 eV represent the doublet states Ti $2p_{1/2}$ and Ti $2p_{3/2}$. The value binding energy difference of two states was 6.4 eV, which was marked for Ti 2p in the anatase TiO_2. The spectrum of O 1s of TiO_2-NFs was from 528 eV to 534 eV, which may be the region with two peaks of 529.5 and 531.3 eV (Figure 5b). The first peak was attributed to the O^{2-} forming oxide with titanium. The remaining energy peak was the O 1s in the C-O band on the surface of the materials [18].

3.3. Photoelectrochemical Performance

The PEC performance of a photocatalyst mainly comes from its structural and morphological properties. The main characteristic of a NF material is a larger surface area which has the corollary of creating numerous places for electron-hole generation [19]. Figure 6 presents photo- and dark-current density and the corresponding photoconversion efficiency for TiO_2-NFs photoelectrodes with different collecting times (5, 10, 15 and 20 min). Figure 6a shows the influence of the spraying time and the applied potential bias on magnitude of photocurrent. Under Xenon lamp illumination, the anodic

photocurrent increased with increasing potential bias for all samples. Corresponding, Figure 6b is the photoconversion efficiency; it shows the increased in photoconversion efficiency when the time is increased and attain a maximum of about 0.03% (corresponding photocurrent density 80 μA/cm^2 at V_{bias} = 0.2 V) at a spraying time of 20 min. This result is comparable or higher than recently reported values for TiO_2 nanostructures [20-22]. We believe that the thickness of the electrode increases with the time, leading to the recombination of a large amount of photogenerated carriers before reaching interface, although a greater quantity of electron-hole pairs was generated. Thus the photoconversion efficiency decreased.

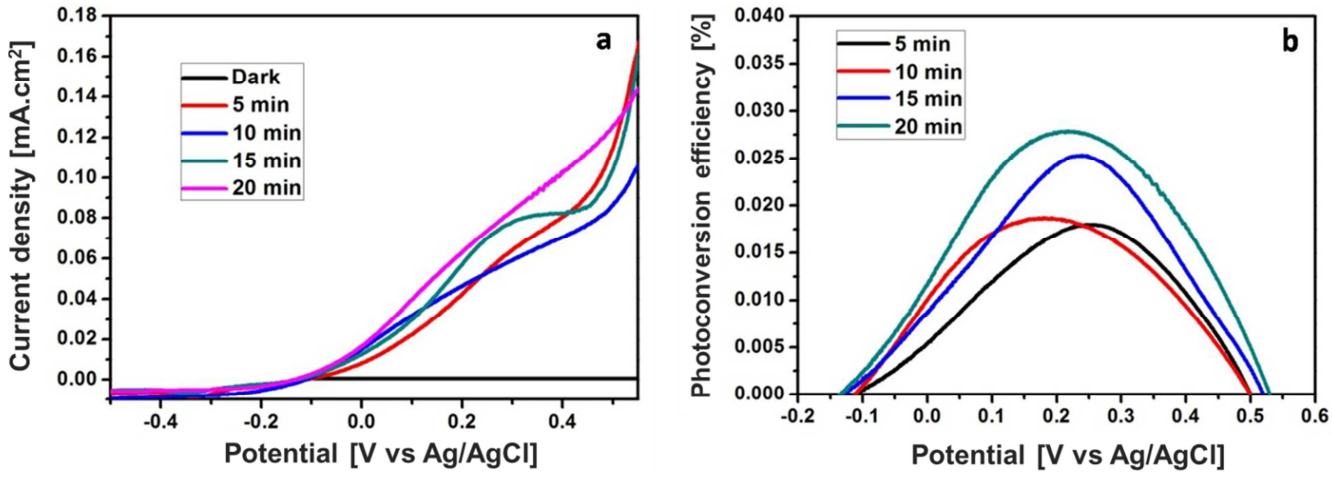

Figure 6. (a) Photo- and dark-current density; (b) Corresponding photoconversion efficiency of TiO_2-NFs with various spraying times.

4. Conclusions

In summary, TiO_2-NFs were successfully prepared by electrospinning in combination with calcination, using as photoanodes in (PEC) for hydrogen generation. The photoconversion efficiency was optimized by controlling the electrode thickness, TiO_2-NFs showing maximum efficiency at 0.03% with 20 min of spraying time under solar light illumination. The results show that the photoanodes using TiO_2-NFs structure is promising for application in energy-to-hydrogen conversion devices.

Acknowledgements

This work is supported by nafosted fund from the Ministry of Science and Technology, Vietnam (Code 103.99-2016.85).

References

[1] M. Ge, J. Cai, J. Iocozzia, C. Cao, J. Huang, X. Zhang, J. Shen, S. Wang, S. Zhang, K. Zhang, Y. Lai, and Z. Lin, "A review of TiO_2 nanostructured catalysts for sustainable H_2 generation," International Journal of Hydrogen Energy 42 (12), 8418-8448 (1972).

[2] J. Y. Huang, S. H. Li, M. Z. Ge, L. N. Wang, T. L. Xing, G. Q. Chen, X. F. Liu, S. S. Al-Deyab, K. Q. Zhang, T. Chen, and Y. K. Lai, "Robust superhydrophobic TiO_2@fabrics for UV shielding, self-cleaning and oil-water separation," J Mater Chem A. 3 (6), 2825-2832 (2015).

[3] J. Nowotny, C. C. Sorrell, R. L. Sheppard, and T. Bak, "Solar-hydrogen: Environmentally safe fuel for the future," International Journal of Hydrogen Energy, 30 (5), 521-544 (2005).

[4] T. Bak, J. Nowotny, M. Rekas, and C. C. Sorrell, "Photoelectrochemical hydrogen generation from water using solar energy: materials-related aspects," Int J Hydrogen Energy 27 (10), 991–1022 (2002).

[5] S. U. M. Khan, M. Al-Shahry, and W. B. Ingler, "Efficient Photochemical Water Splitting by a Chemically Modified N-TiO_2,". Science 297 (5590), 2243–2245 (2002).

[6] Fujishima and K. Honda, "Electrochemical Photolysis of Water at a Semiconductor Electrode," Nature 238, 37-38 (1972).

[7] L. Zeng, Z. Lu, M. H. Li, J. Yang, W. L. Song, D. W. Zeng, and C., Xie, "A modular calcination method to prepare modified N-doped TiO_2 nanoparticle with high photocatalytic activity," Appl Catal B-Environ 183, 308-316 (2016).

[8] H. Y. Chuang and D. H. Chen, "Fabrication and photoelectrochemical study of Ag@TiO_2 nanoparticle thin film electrode," Int J Hydrogen Energy 36 (16), 9487-9495 (2011).

[9] B. Liu, J. Z. Xiao, L. Xu, Y. J. Ya, B. F. O. Costa, V. F. Domingos, E. S. Ribeiro, F. N. Shi, K. Zhou, J. Su, H. Wu, K. Zhong, J. A. Paixao, and J. M. Gil, "Gelatin-assisted sol-gel derived TiO_2 microspheres for hydrogen storage," Int J Hydrogen Energy 40 (14), 4945-4950 (2015).

[10] Y. Xia, P. Yang, Y. Sun, Y. Wu, B. Mayers, B. Gates, Y. Yin, F. Kim, and H. Yan, "One-Dimensional Nanostructures: Synthesis, Characterization, and Applications," Advanced Materials 15 (5), 353–389 (2003).

[11] R. Sui, A. S. Rizkalla, and P. A. Charpentier, "Formation of Titania Nanofibers: A Direct Sol-Gel Route in Supercritical CO_2," Langmuir 21 (14), 6150–6153 (2005).

[12] B. Caratão, E. Carneiro, P. Sá, B. Almeida, and S. Carvalho, "Properties of Electrospun TiO_2 Nanofibers," J. Nanotech, 2014 (2), 472132 (2014).

[13] C. H. Chang, H. C. Lee, C. C. Chen, Y. H. Wu, Y. M. Hsu, Y. P. Chang, T. I. Yang, and H. W. Fang, "A Novel Rotating Electrochemically Anodizing Process to Fabricate Titanium Oxide Surface Nanostructures Enhancing the Bioactivity of Osteoblastic Cells," J. Bio. Mat. Res. - Part A, 100 (7), 1687–1695 (2012).

[14] Tavangar, B. Tan, and K. Venkatakrishnan, "Study of the Formation of 3-D Titania Nanofibrous Structure by MHz Femtosecond Laser in Ambient Air," Journal of Applied Physics 113 (2), 9 (2013).

[15] H. Wang, Y. Liu, M. Zhong, H. Xu, H. Huang, and H. Shen, "In Situ Controlled Synthesis of Various TiO_2 Nanostructured Materials via a Facile Hydrothermal Route". Journal of Nanoparticle Research 13 (5), 1855–1863 (2011).

[16] H. N. Hieu, N. Q. Dung, J. Kim, and D. Kim, "Urchin-like nanowire array: a strategy for high-performance ZnO-based electrode utilized in photoelectrochemistry," Nanoscale, 5 (12), 5530-5538 (2013).

[17] W. Nuansing, S. Ninmuang, W. Jarernboon, S. Maensiri, and S. Seraphin, "Structural Characterization and Morphology of Electrospun TiO_2 nanofibers," Materials Science and Engineering B: Solid-State Materials for Advanced Technology 131 (1–3), 147–155 (2006).

[18] S. Chaguetmi, F. Mammeri, M. Pasut, S. Nowak, H. Lecoq, P. Decorse, C. Costentin, S. Achour, and S. Ammar, "Synergetic Effect of CdS Quantum Dots and TiO_2 Nanofibers for Photoelectrochemical Hydrogen Generation," J. Nano. Res. 15 (12), 10 (2013).

[19] N. Sobti, A. Bensouici, F. Coloma, C. Untiedt, and S. Achour, "Structural and photoelectrochemical properties of porous TiO_2 nanofibers decorated with Fe_2O_3 by sol-flame," J. Nanopart. Res. 16, 2577 (2014).

[20] L. Li, H. Dai, L. Feng, D. Luo, S. Wang, and X. Sun, "Enhance Photoelectrochemical Hydrogen-Generation Activity and Stability of TiO_2 nanorod Arrays Sensitized by PbS and CdS Quantum Dots under UV-Visible Light," Nano. Res. Let. 10 (1), 48 (2015).

[21] Y. Li, F. Gao, L. Zhao, Y. Ye, J. Liu, and Y. Tao, "Reversing CdS and ZnS Preparation Order on Electrospun TiO_2 and Its Effects on Photoelectrochemical Property," Micro & Nano Letters 11, 731–733 (2016).

[22] J. Krysa, M. Zlamal, S. Kment, M. Brunclikova, and Z. Hubicka, "TiO_2 and Fe_2O_3 Films for Photoelectrochemical Water Splitting," Molecules 20 (1), 1046–1058 (2015).